J|A|C|S COMMUNICATIONS

Published on Web 11/13/2009

Selective Imaging of Damaged Bone Structure (Microcracks) Using a Targeting Supramolecular Eu(III) Complex As a Lanthanide Luminescent Contrast Agent

Brian McMahon,[†] Peter Mauer,[‡] Colin P. McCoy,[§] T. Clive Lee,[‡] and Thorfinnur Gunnlaugsson*,[†]

School of Chemistry, Center for Synthesis and Chemical Biology, Trinity College Dublin, Dublin 2, Ireland, Department of Anatomy, Royal College of Surgeons in Ireland, St. Stephen's Green, Dublin 2, Ireland, and School of Pharmacy, Queen's University of Belfast, 97 Lisburn Road, Belfast, BT9 7BL U.K.

Received September 21, 2009; E-mail: gunnlaut@tcd.ie

The sensing and imaging of biological matter using lanthanide luminescent supramolecular sensors,[1,2] or imaging agents,[3,4] has attracted significant attention in recent years. The photophysical properties of ions such as Eu(III) and Tb(III), which possess long-lived excited states and line-like emission bands, occurring at long wavelengths, makes these ions excellent candidates for use in such applications, as they overcome short-lived background emission and light scattering from biological matter.[5,6] To date, lanthanide complexes have been designed for both luminescent cellular and tissue imaging.[7] However, the development of such luminescent agents for larger biological structures, such as bones,[8] has, to the best of our knowledge, not been achieved to date.

Bone is a rigid structure consisting of canals, Haversian systems, canaliculi, and resorption cavities. Being a dynamic organ it undergoes continuous repair, shaping, and molding.[9] The formation of microcracks in bones (25−300 μm in length in human bones) is usually caused by repetitive loading and stress and can have extreme biological effects and hence medical conditions, such as osteoporosis.[10] Due to the presence of organic matrix and crystalline hydroxyapatite in bones, it can be difficult to distinguish such damage from healthy bone. Hence, the development of novel contrast agents which have the ability to penetrate the bone matrix can enable a greater understanding of this complex morphology.[10,11] Herein we present an example of a luminescent lanthanide bone-targeting imaging agent,[12] **1.Eu.Na**, designed for the selective Eu(III) imaging of damaged bone at physiological pH. We foresaw that **1.Eu.Na**, which possess three iminodiacetate moieties,[12] would be able to bind selectively to exposed Ca(II) sites within the hydroxyapaptite lattice of the bone, enabling the luminescent imaging of this exposed damage.

The synthesis of **1.Eu.Na**, Scheme 1, was achieved in few steps from **2**,[13] which was reacted with 3 equiv of diethyl 2,2-(2-chloroacetyl-amino)diacetate, **3**, in refluxing MeCN solution, in the presence of Et_3N for 7 days. Purification using alumina column chromatography (gradient elution 100→80:20 CH_2Cl_2/CH_3OH) afforded **1** in 54% yield, which was reacted with 1 equiv of $Eu(CF_3SO_3)_3$ in freshly distilled MeCN for 15 h (Figure S1b), giving **1.Eu** in 69% yield (see ^{1}H NMR in Figure S1). Alkaline hydrolysis of **1.Eu** in MeOH/H_2O gave **1.Eu.Na** in 90% yield after precipitation from dry diethyl ether.

The design of **1.Eu.Na** envisaged indirect excitation of the Eu(III) ion via the covalently attached naphthalene antenna, enabling the sensitization of the Eu(III) $^5D_0$ excited state, which upon relaxation to the ^7F_J ($J = 0, 1, 2, 3, 4$) ground state gives rise to characteristic line-like Eu(III) emission.[1,5] Indeed, metal centered emissions occurring at 580, 595, 616, 655, and 701 nm (Figure S2) were observed in

Scheme 1. Synthesis of **1** (Free Ligand) and Corresponding Eu(III) Complexes **1.Eu** and **1.Eu.Na**

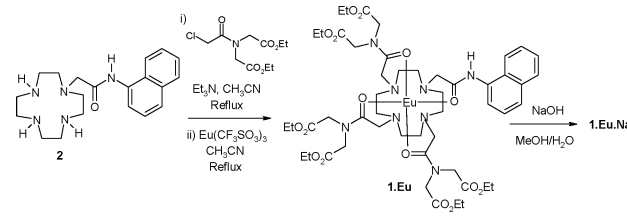

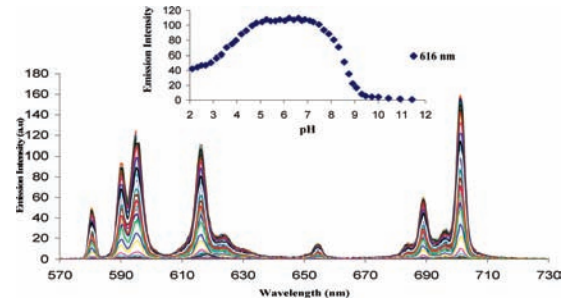

Figure 1. Changes in the Eu(III) luminescence of **1.Eu.Na** upon excitation of the naphthalene antenna as a function of pH ($I = 0.1$ M NEt_4HClO_4 (TEAP)). Insert: The changes at 616 nm vs pH.

aqueous buffered pH 7.4 (20 mM HEPES) solution upon excitation at the antenna, as well as upon direct excitation of the metal center of both **1.Eu** and **1.Eu.Na**. The excited state lifetimes in H_2O and D_2O, upon excitation at 282 nm, gave $\tau_{H_2O} = 0.576$ ms and $\tau_{D_2O} = 1.744$ ms from which the hydration state $q \approx 1$ (Figure S3) was determined, indicating that **1.Eu.Na** possessed one metal bound water molecule, the Eu(III) ion being overall nine coordinated. The effect of pH on both the ground and the singlet excited states of the antenna and the Eu(III) excited states were analyzed so as to quantify the pH dependence of **1.Eu.Na** within the physiological pH range. While the pH dependence changes in the absorption spectra of **1.Eu.Na** (Figure S4a) were minor, the fluorescence emission (Figure S4b) and the Eu(III) emission, Figure 1, were significantly modulated as a function of pH ($\lambda_{EX} = 282$ nm). The analysis of the Eu(III) emission for the $\Delta J = 2$ transition (see inset in Figure 1) clearly demonstrates that the Eu(III) emission was *'switched on'* within the physiological pH range, being only *'switched off'* below pH 5 or above pH 8.[14] To further investigate the effectiveness of **1.Eu.Na** as a potential contrast agent, its luminescence response toward group I and II as well as several biologically relevant *d*-metal ions was determined (as their MCl_2 salts) within the concentration range 0−0.1 mM in buffered pH = 7.4 (20 mM HEPES) solution. In general, only minor changes were observed in the Eu(III) emission of **1.Eu.Na** (Figures S5−S10), in the presence

[†] Trinity College Dublin.
[‡] Royal College of Surgeons in Ireland.
[§] Queen's University of Belfast.

10.1021/ja908006r

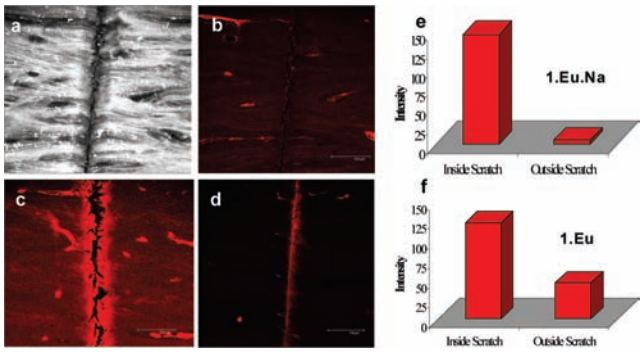

Figure 2. Confocal laser-scanning microscopy images of bone sample immersed in a 1×10^{-3} M solution of **1.Eu.Na** (pH 7.4, 20 mM HEPES, 135 mM KCl): (a) Reflected light image: 0 h, (b) Control, (c) 4 h, (d) 24 h. Bar = 150 μm. (e) Contrast between Eu(III) emission from **1.Eu.Na** inside and outside the scratch after 24 h. (f) The contrast observed using **1.Eu** (1×10^{-3} M) after 24 h.

of these ions, with the exception of Co(II) and Ni(II) (Figures S9−10) which resulted in quenching of the Eu(III) emission.

We next evaluated the ability of **1.Eu.Na** to act as a luminescent imaging agent for bone cracks. To demonstrate this, several bovine tibia specimens were sectioned and polished to give mechanically smooth surfaces (see Supporting Information), which should have low or no affinity for **1.Eu.Na** and, hence, would not result in positive luminescent imaging of such areas. The same samples were then scratched using established protocols,[11,12] exposing fresh Ca(II) sites. These specimens were then treated with a 1×10^{-3} M aqueous solution of **1.Eu.Na** (in 135 mM of KCl at pH 7.4) for a period of 0 to 24 h. For comparison, polished and scratched bone samples were also treated with **1.Eu**. Using steady-state fluorescence, the Eu(III) emissions from the samples containing 'smooth' and scratched bone surfaces were first recorded using specimens that were stained for 4 and 24 h. The results clearly demonstrated that the Eu(III) emission from the scratched areas was more intense than that of the undamaged surface, with all of the $^5D_0 \rightarrow {}^7F_J$ transitions being clearly visible, even after 4 h of staining. Similarly, using **1.Eu**, some Eu(III) emission was also visible. However, in comparison to **1.Eu.Na**, the emission was significantly less visible (Figures S11−12). Furthermore, by analyzing the intensity ratios of the various Eu(III) ΔJ transitions, it was clear that the ratio between $\Delta J = 1$ and 2 was significantly greater for **1.Eu** than for **1.Eu.Na**, for which the ratio was almost 1:1. This would suggest that **1.Eu** bound to the scratched surface in a different manner to **1.Eu.Na**, which is to be expected, as in **1.Eu** the Ca(II) chelating moieties are blocked.

The samples were next imaged using confocal fluorescence laser-scanning microscopy. The overall results are shown in Figure 2 (Figure 2a shows the bone scratch as a reflected light image), where in Figure 2c and 2d the emission (recorded at 616 nm) arising from the bone surface of the same sample after 4 and 24 h staining/exposure to **1.Eu.Na** is clearly visible, being most pronounced within the scratched areas. In contrast, Figure 2b shows no such emission arising from a bone surface that was exposed to **1.Eu.Na** for 24 h, after which it was scratched and imaged. Hence, the presence of exposed Ca(II) sites is a prerequisite for the successful binding of **1.Eu.Na** to the bone surface and, hence, imaging of any damaged bone surface. It is also clear from Figure 2b−d that the emission contrast between the healthy bone surface and the scratched areas enhances significantly with increasing **1.Eu.Na** exposure time. While Figure 2c shows that the Eu(III) emission from the crack is clearly distinguishable from the surrounding undamaged bone after only 4 h of exposure, where the intensity enhancement (IE) (at 616 nm) within the scratched area is only twice that measured for the unscratched area. In contrast, after 24 h of exposure, Figure 2d, the emission from the healthy bone surface is almost negligible (in comparison to the scratched surface), with an IE $\approx$ 28, Figure 2e, making the distinction between healthy and damaged bone clear.

The images shown in Figure 2b−d clearly demonstrate the ability of **1.Eu.Na** to selectively bind and hence image the damaged bone sites, likely occurring through chelation to exposed Ca(II) sites within these cracks. To confirm this, the ability of **1.Eu** to bind to such scratched bone regions was also investigated. The confocal fluorescence laser-scanning microscopy images (Figure S13) indeed showed that **1.Eu** did bind to the scratched areas. However, the contrasting ability is much diminished relative to **1.Eu.Na**, with an EI of only 2 being determined after 24 h of exposure (Figure 2f), an order of magnitude smaller IE than that for **1.Eu.Na**. Furthermore, unlike the case for **1.Eu.Na**, no significant change was seen in the Eu(III) emission intensity between samples exposed to **1.Eu** for 4 and 24 h, respectively (Figure S14). This clearly highlights the important role that the iminodiacetate moieties in **1.Eu.Na** play to selectively bind the agent to the damaged hydroxyapaptite lattice, resulting in effective imaging of such bone damage.

In summary, we have developed the first example of a cyclen based Eu(III) complex, incorporating the iminodiacetate functionalities (as selective Ca(II) binding motifs), as a lanthanide luminescent contrast agent for bone structure analysis. We are in the process of further studying the properties of **1.Eu.Na** and other related Eu(III) and Gd(III) structures as bone imaging agents.

Acknowledgment. We thank IRCSET (Postgraduate award to B.M.), TCD, QUB, and RCSI for financial support and The University of Canterbury, New Zealand, for a 2009 Erskine Fellowship to T.G.

Supporting Information Available: Synthesis and characterization of all novel compounds, Figures S1−13. This material is available free of charge via the Internet at http://pubs.acs.org.

References

(1) (a) dos Santos, C. M.G.; Harte, A. J.; Quinn, S. J.; Gunnlaugsson, T. *Coord. Chem. Rev.* **2008**, *252*, 2512. (b) Leonard, J. P.; Nolan, C. B.; Stomeo, F.; Gunnlaugsson, T. *Top. Curr. Chem.* **2007**, *281*, 1. (c) Gunnlaugsson, T.; Stomeo, F. *Org. Biomol. Chem.* **2007**, *5*, 1999.
(2) (a) Nonat, A. M.; Quinn, S. J.; Gunnlaugsson, T. *Inorg. Chem.* **2009**, *48*, 4646. (b) Massue, J.; Quinn, S. J.; Gunnlaugsson, T. *J. Am. Chem. Soc.* **2008**, *130*, 6900. (c) Plush, S. E.; Gunnlaugsson, T. *Dalton Trans.* **2008**, 3801.
(3) (a) Bünzli, J.-C. G. *Chem. Lett.* **2009**, *38*, 104. (b) Song, B.; Vandevyver, D. B.; Deiters, E.; Chauvin, A.-S.; Hemmila, I.; Bünzli, J.-C. G. *Analyst* **2008**, *133*, 1749.
(4) (a) Pandya, S.; Yu, J.; Parker, D. *Dalton Trans.* **2006**, 2757. (b) Yu, J. J.; Parker, D.; Pal, R.; Poole, R. A.; Cann, M. J. *J. Am. Chem. Soc.* **2006**, *128*, 2294.
(5) Gunnlaugsson, T.; Leonard, J. P. *Chem. Commun.* **2005**, 3114.
(6) (a) Montgomery, C. P.; Murray, B. S.; New, E. J.; Pal, R.; Parker, D. *Acc. Chem. Res.* **2009**, *47*, 925. (b) Thibon, A.; Pierre, V. C. *Anal. Bioanal. Chem.* **2009**, *394*, 107. (c) Motson, G. R.; Fleming, J. S.; Brooker, S. *Adv. Inorg. Chem.* **2004**, *55*, 361.
(7) (a) Deiters, E.; Song, B.; Chauvin, A. S.; Vandevyver, C. D. B.; Gumy, F.; Bünzli, J. C. G. *Chem.—Eur. J.* **2009**, *15*, 885. (b) Chauvin, A. S.; Comby, S.; Song., B.; Vandevyver, C. D. B.; Bünzli, J. C. G. *Chem.—Eur. J.* **2008**, *14*, 1726.
(8) Examples of Gd(III) MRI contrast agents for bone targeting include: (a) Vitha, T.; Kubicek, V.; Kotek, J.; Hermann, P.; Elst, L. V.; Muller, R. N.; Lukes, I.; Peters, J. A. *Dalton Trans.* **2009**, 3204. (b) Kubicek, V.; Rudovsky, J.; Kotek, J.; Hermann, P.; Elst, L. V.; Muller, R. N.; Kolar, Z. I; Wolterbeek, H. T; Peters, J. A; Lukes, I. *J. Am. Chem. Soc.* **2005**, *127*, 16477.
(9) Lee, T. C.; Mohsin, S.; Taylor, D.; Parkesh, R.; Gunnlaugsson, T.; O'Brien, F. J.; Giehl, M.; Gowin, W. *J. Anat.* **2003**, *203*, 161.
(10) Taylor, D.; Hazenberg, J. G.; Lee, T. C. *Nat. Mater.* **2007**, *6*, 263.
(11) (a) Parkesh, R.; Mohsin, S.; Lee, T. C.; Gunnlaugsson, T. *Chem. Mater.* **2007**, *19*, 1656. (b) Parkesh, R; Gowin, W.; Lee, T. C.; Gunnlaugsson, T. *Org. Biomol. Chem.* **2006**, *4*, 3611.
(12) Parkesh, R.; Lee, T. C.; Gunnlaugsson, T. *Tetrahedron Lett.* **2009**, *50*, 4114.
(13) Plush, S. E.; Gunnlaugsson, T. *Org. Lett.* **2007**, *9*, 1919.
(14) Gunnlaugsson, T.; Leonard, J. P.; Sénéchal-David, K.; Harte, A. J. *J. Am. Chem. Soc.* **2003**, *125*, 12062.

JA908006R